PROCEEDINGS OF SCIENCE

Towards Understanding the Origin of Cosmic-Ray Positrons and Electrons

Zhili Weng[†,*]

Massachusetts Institute of Technology, Cambridge, USA

E-mail: zhili.weng@cern.ch

Precision measurements of cosmic-ray positron flux and electron flux by the Alpha Magnetic Spectrometer on the International Space Station are presented based on 1.9 million positrons up to 1 TeV and 28.1 million electrons up to 1.4 TeV. The positron flux and electron flux have distinctly different magnitudes and energy dependences. The positron flux exhibits a significant excess starting from 25.2 ± 1.8 GeV followed by a sharp drop-off above 284^{+91}_{-64} GeV. In the entire energy range, the positron flux is well described by the sum of a diffuse term associated with low energy secondary positrons produced in the collision of cosmic rays, and a new source term of high energy positrons with a finite energy cutoff. The finite cutoff energy of the source term, E_s, is determined to be 810^{+310}_{-180} GeV, with a significance of more than 4σ. The electron flux exhibits a significant excess starting from $42.1^{+5.4}_{-5.2}$ GeV compared to the lower energy trends, but the nature of this excess is different from the positron flux excess. Below 1.9 TeV, the electron flux does not have an exponential energy cutoff at more than 5σ level. These experimental data show that, at high energies, positrons predominantly originate either from dark matter collisions or from new astrophysical sources, whereas most high energy electrons originate from different sources than high energy positrons.

40th International Conference on High Energy physics - ICHEP2020
July 28 - August 6, 2020
Prague, Czech Republic (virtual meeting)

[†]On behalf of the AMS Collaboration
[*]Speaker

PoS(ICHEP2020)615

Studies of cosmic-ray positrons and electrons are crucial for the understanding of new physics phenomena in the universe. There has been widespread interests and various explanations [1–4] of the observed excess of high energy positrons [5]. Most of these explanations differ in their predictions for the behavior of cosmic ray positrons and electrons at high energies.

In this proceeding, we present precision measurements of the positron flux and electron flux by the Alpha Magnetic Spectrometer (AMS) on the International Space Station (ISS). The description of the AMS detector, as well as the analysis procedures for electrons and positrons, are described in detail in Ref. [6, 7] and references therein. The key detector elements used for these analyses are the transition radiation detector TRD, the time of flight counters TOF, the silicon tracker, the permanent magnet, and the electromagnetic calorimeter ECAL. The combination of information from the TRD, tracker, and ECAL enables the precision identification and measurement of 1.9 million positrons from 0.5 GeV to 1 TeV, and 28.1 million electrons from 0.5 GeV to 1.4 TeV. These measurements reveal distinctive properties of positron flux and electron flux, providing new insights into new physics phenomena in the cosmos.

1. Distinctive Properties of Positron Flux

The AMS positron spectrum (defined as the flux scaled by E^3) [6] is presented in Figure 1. The spectrum exhibits complex energy dependence: it is flattening from 7.10 to 27.25 GeV (green vertical band); from 27.25 to 290 GeV the positron spectrum exhibits significant rise (orange vertical band); at ~290 GeV the positron spectrum reaches a maximum followed by a sharp drop-off (blue vertical band). The time variation of the flux at low energies due to solar modulation is indicated by the red band.

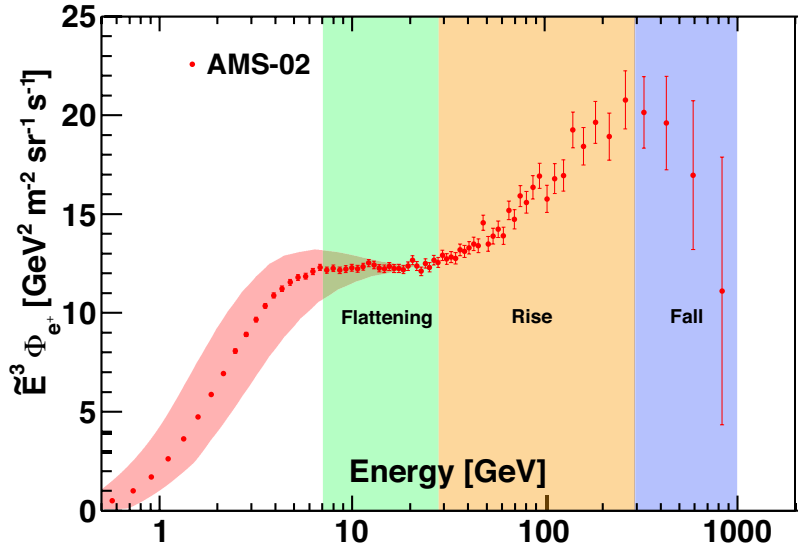

Figure 1: The positron spectrum, $\tilde{E}^3\,\Phi_{e^+}$, (red data points) is shown as a function of energy.

To determine the transition energy E_0 where the positron flux changes its behavior, we use a double power-law function :

$$\Phi(E) = \begin{cases} C(E/55.58\,\text{GeV})^{\gamma}, & E \le E_0; \\ C(E/55.58\,\text{GeV})^{\gamma}(E/E_0)^{\Delta\gamma}, & E > E_0. \end{cases} \quad (1)$$

where γ is the spectral index below E_0 and $\Delta\gamma$ is the change of the spectral index above E_0. A fit to the data in the energy range $[7.10 - 55.58]$ GeV yields $E_0 = 25.2 \pm 1.8$ GeV for the energy where the spectral index increases ($\Delta\gamma > 0$). As presented in Fig. 2 a), this indicates a significant excess of the positron flux compared to the lower energy trends. In the energy range $[55.58 - 1000]$ GeV, the fit yields $E_0 = 284^{+91}_{-64}$ GeV for the energy of the spectral index decrease ($\Delta\gamma < 0$), as presented in Fig. 2 b).

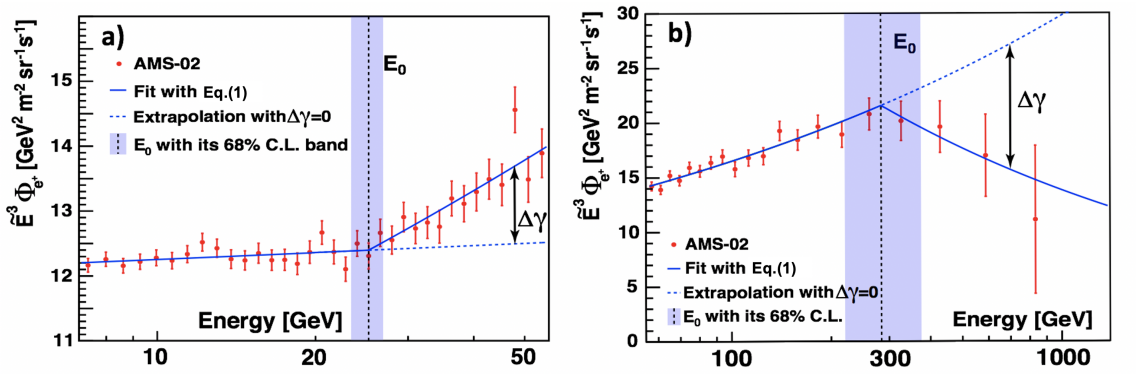

Figure 2: The double power-law fits of Eq. (1) to the positron flux in the energy ranges $[7.10 - 55.58]$ GeV and $[55.58 - 1000]$ GeV, respectively.

At energy starting from $\sim$ 10 GeV, the AMS positron flux by far exceeds the contribution from secondary positrons produced from the collision of cosmic rays with the interstellar gas [8], a primary source of positrons is needed to describe the observed positron excess. Models to explain the primary source of cosmic-ray positrons include annihilation of dark matter particles [2] and other astrophysical objects like supernova remnants or pulsars [3].

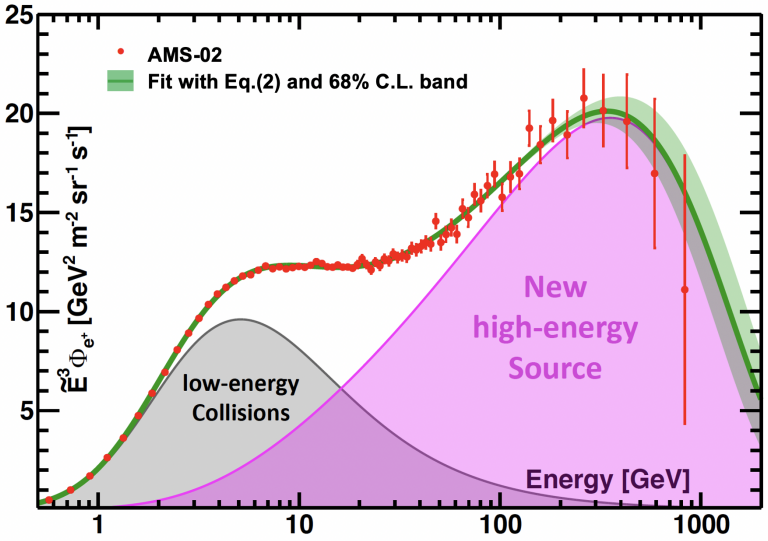

Figure 3: The fit of Eq. (2) (green line) to the positron flux in the energy range $[0.5 - 1000]$ GeV together with the 68% C.L. interval (green band). The source term contribution is represented by the magenta area, and the diffuse term contribution by the grey area.

The accuracy of the AMS data allows for a detailed study of the properties of the new source of positrons. For example, the positron flux can be parametrized as the sum of a diffuse term and a

source term:

$$\Phi_{e^+}(E) = \frac{E^2}{\hat{E}^2}[C_d\,(\hat{E}/E_1)^{\gamma_d} \;+\; C_s\,(\hat{E}/E_2)^{\gamma_s}\,\exp(-\hat{E}/E_s)]\,. \tag{2}$$

The diffuse term is a power-law function, which describes the secondary positrons produced in the collisions of primary cosmic rays with the interstellar gas. The source term is a power-law function with an exponential cutoff, which describes the high energy part of the flux dominated by a source. The force-field approximation [9] is used to account for solar modulation effect. A detailed description of the parameters and their fitted values can be found in Ref. [6]. The fit of Eq. (2) to the measured flux yields the cutoff energy $E_s = 810^{+310}_{-180}$ GeV and χ^2/d.o.f. = 50/68. The cutoff energy E_s at infinity is excluded at a significance of 4.07σ. The result of the fit is presented in Fig. 3. As seen, the diffuse term (grey filled area) dominates at low energies and gradually vanishes with increasing energy. The source term (magenta filled area) dominates the positron spectrum at high energies.

These experimental data on cosmic-ray positrons show that, at high energies, they predominantly originate either from dark matter annihilation or from other astrophysical sources.

2. Distinctive Properties of Electron Flux

The latest precision measurement by AMS on the cosmic-ray electron flux up to 1.4 TeV reveal new features. As shown in Figure 4, over the entire energy range, the electron spectrum is distinctly different from the positron spectrum in magnitudes and energy dependences.

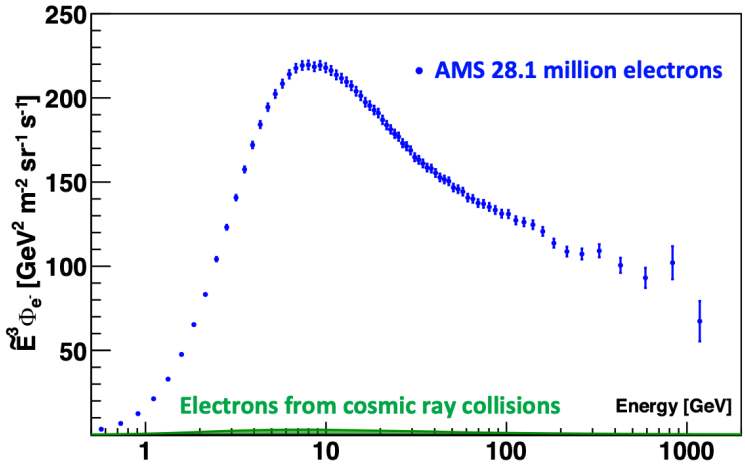

Figure 4: The AMS electron spectrum ($\tilde{E}^3\Phi_{e^-}$, blue data points) together with the GALPROP prediction for secondary electrons.

We examine the changing behavior of the electron flux using the double power-law approximation (Eq. (1)). A fit to the data in the energy range [20.04 − 1400] GeV yields $E_0 = 42.1^{+5.4}_{-5.2}$ GeV for the energy where the electron spectrum changes its behavior, with $\Delta\gamma = 0.094 \pm 0.014$, indicating an excess of the electron flux compared to the lower energy trends.

Above 41.61 GeV, the electron flux can be described by a power-law function. A fit to the data above this energy using the function $\Phi_{e^-}(E) = C_s\,(E/41.61\,\text{GeV})^{\gamma_s}\,\exp(-E/E_s)$ yields the inverse cutoff energy $1/E_s = 0.00^{+0.08}_{-0.00}$ TeV^{-1}. Further study of the cutoff energy shows that $E_s < 1.9$ TeV is excluded at more than 5σ significance.

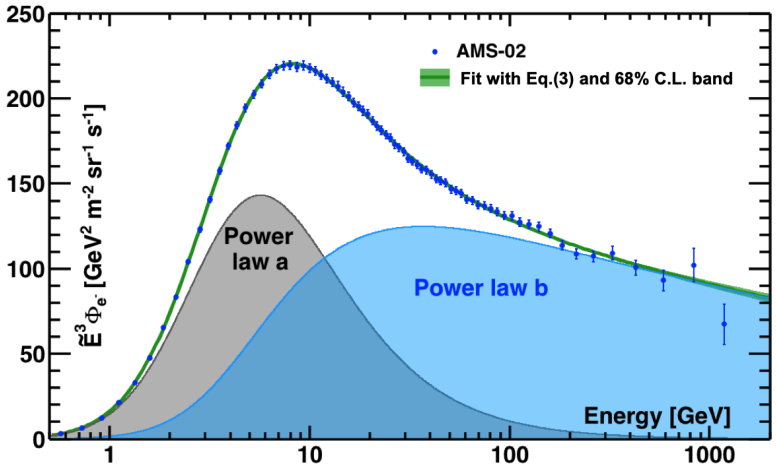

Figure 5: The two-power-law fit (Eq. (3)) to the electron flux data in the energy range [0.5 – 1400] GeV with the 68% C.L. (green band). The two power-law components a and b are represented by the gray and blue areas, respectively.

New sources of high energy positrons, such as dark matter, may produce an equal amount of high energy electrons and positrons. This hypothesis is tested using the source term from the positron fit. (Eq. (2)). Above 41.61 GeV, the electron flux is consistent with the existence of a high energy electron source term identical to that of positrons, while also consistent with the absence of such a term. Future AMS measurements with increased accuracy and extended energy reach will enable us to ascertain the existence of the source term contribution to the electron flux.

As seen in Figure 4, the contribution of the collision of cosmic rays [8] to the electron spectrum is negligible. There could be several astrophysical sources of primary cosmic-ray electrons [10]. In addition, there are several physics effects that may introduce spectral features in the flux [11]. We studied the minimal number of distinct power-law functions to accurately describe the AMS electron flux and concluded that in the entire energy range [0.5 – 1400] GeV the electron flux is well described by the sum of two power-law components:

$$\Phi_{e^-}(E) = \frac{E^2}{\hat{E}^2}[1 + (\hat{E}/E_t)^{\Delta\gamma_t}]^{-1}[C_a(\hat{E}/E_a)^{\gamma_a} + C_b(\hat{E}/E_b)^{\gamma_b}]. \quad (3)$$

The two components, a and b, correspond to two power-law functions. The force-field approximation [9] is used to account for solar modulation effect. At low energy, an additional transition term is introduced to account for complex spectral behavior below $\sim$ 10 GeV. A detailed discussion of the parameters and their fitted values can be found in Ref. [7]. The fit to the data in the energy range [0.5 – 1400] GeV is presented in Figure 5. As seen, the sum of two power-law functions with the additional transition term provides an excellent description of the data. These functions are very different in shape and in magnitude from those describing the positron flux and indicate that most cosmic-ray electrons originate from different sources than cosmic-ray positrons.

3. Conclusion

Precision measurements of the cosmic-ray positron flux and electron flux by AMS are presented based on 1.9 million positrons up to 1 TeV and 28.1 million electrons up to 1.4 TeV. The electron flux

and positron flux have distinctly different magnitudes and energy dependences. These experimental data show that at high energies, cosmic-ray positrons predominantly originate either from dark matter collisions or from new astrophysical sources. The different behavior of the cosmic-ray electron flux and positron flux is clear evidence that most high energy electrons originate from different sources than high energy positrons. AMS will continue to improve the accuracy and the energy reach of the measurements on positron flux and electron flux, so as to determine the origin of high energy cosmic-ray positrons and electrons.

References

[1] F. Donato, N. Fornengo, and P. Salati, Phys. Rev. D **62** 043003 (2000); M. Cirelli, R. Franceschini, and A. Strumia, Nucl. Phys. B **800**, 204 (2008); P. Blasi. Phys. Rev. Lett. **103** 051104 (2009);

[2] M. S. Turner and F. Wilczek, Phys. Rev. D **42** 1001 (1990); J. Ellis, AIP Conf. Proc. **516**, 21 (2000); J. Kopp, Phys. Rev. D 88, 076013 (2013); L. Bergstrom *et al.*, Phys. Rev. Lett. 111, 171101 (2013);

[3] P. D. Serpico, Astropart. Phys. **39-40** 2 (2012); T. Linden and S. Profumo, Astrophys. J. **772**, 18 (2013); P. Mertsch and S. Sarkar, Phys. Rev. D **90**, 061301 (2014); I. Cholis and D. Hooper, Phys. Rev. D 88, 023013 (2013);

[4] R. Cowsik, B. Burch, and T. Madziwa-Nussinov, Astrophys. J. **786**, 124 (2014); K. Blum, B. Katz, and E. Waxman, Phys. Rev. Lett. **111**, 211101 (2013).

[5] M. Aguilar *et al.*, Phys. Rev. Lett. **110**, 141102 (2013); L. Accardo *et al.*, Phys. Rev. Lett. **113**, 121101 (2014). M. Aguilar *et al.*, Phys. Rev. Lett. **113**, 121102 (2014); M. Aguilar *et al.*, Phys. Rev. Lett. **113**, 221102 (2014).

[6] M. Aguilar *et al.*, Phys. Rev. Lett. **122**, 041102 (2019).

[7] M. Aguilar *et al.*, Phys. Rev. Lett. **122**, 101101 (2019).

[8] I. V. Moskalenko and A. W. Strong, Astrophys. J. **493**, 694 (1998); A. E. Vladimirov, S. W. Digela, G. Jóhannesson, P. F. Michelson, I. V. Moskalenko, P. L. Nolan, E. Orlando, T. A. Porter, and A. W. Strong, Comput. Phys. Commun. **182**, 1156 (2011). R. Trotta, G. Johannesson, I. Moskalenko, T. Porter, R. Ruiz de Austri, and A. Strong, Astrophys. J. **729**, 106 (2011).

[9] L. Gleeson and W. Axford, Astrophys. J. **154**, 1011 (1968).

[10] A.M. Hillas, J. Phys. G: Nucl. Part. Phys. **31**, R95 (2005); Y.Z. Fan, B. Zhang, and J. Chang, Int. J. Mod. Phys. D **19**, 2011 (2010).
T. Kobayashi, Y. Komori, K. Yoshida, and J. Nishimura, Astrophys. J. **601**, 340 (2004).

[11] Ł. Stawarz, V. Petrosian, and R. D. Blandford, Astrophys. J. **710**, 236 (2010).
A.W. Strong, E. Orlando, and T.R. Jaffe, Astron. Astrophys. **534**, A54 (2011).